

# View Vertically: A Hierarchical Network for Trajectory Prediction via Fourier Spectrums

Conghao Wong, Beihao Xia, Ziming Hong, Qinmu Peng,  
and Xinge You, *Senior Member, IEEE*

**Abstract**—Learning to understand and predict future motions or behaviors for agents like humans and robots are critical to various autonomous platforms, such as behavior analysis, robot navigation, and self-driving cars. Intrinsic factors such as agents' diversified personalities and decision-making styles bring rich and diverse changes and multi-modal characteristics to their future plannings. Besides, the extrinsic interactive factors have also brought rich and varied changes to their trajectories. Previous methods mostly treat trajectories as time sequences, and reach great prediction performance. In this work, we try to focus on agents' trajectories in another view, i.e., the Fourier spectrums, to explore their future behavior rules in a novel hierarchical way. We propose the Transformer-based V model, which concatenates two continuous keypoints estimation and spectrum interpolation sub-networks, to model and predict agents' trajectories with spectrums in the keypoints and interactions levels respectively. Experimental results show that V outperforms most of current state-of-the-art methods on ETH-UCY and SDD trajectories dataset for about 15% quantitative improvements, and performs better qualitative results.

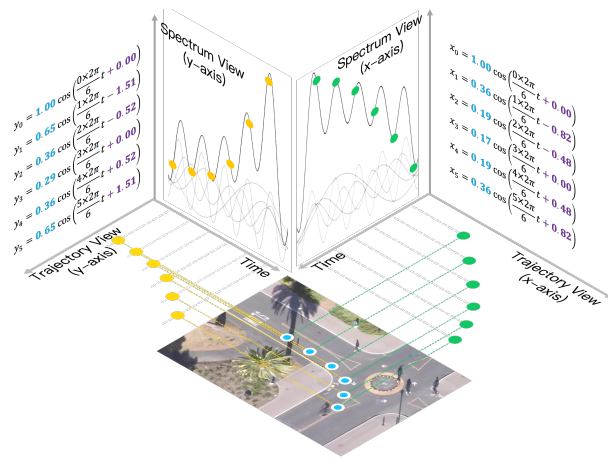


Fig. 1. We show the trajectory in two views, the time sequences view and the Fourier spectrums view. The x-axis trajectory (green dots) and the y-axis trajectory (yellow dots) have similar “shapes”, while they are quite different in the spectrum views (shown with amplitudes and phases).

## 1 INTRODUCTION

Trajectory prediction is a novel but essential task, which can be applied to behavior analysis, robot navigation, autonomous driving, tracking, detection, and many other computer vision tasks or applications. It aims at inferring agents' possible future trajectories in crowd spaces considering multiple potential factors. Agents' future plans can be easily affected by various kinds of factors, including both intrinsic factors (like various personalities or different preferences) and extrinsic factors (like interactions or

constraints among agents and environments). The diversity and uncertainty of agents, scenes, and interactive behaviors have also brought enormous challenges. In addition, the modeling and description of the structured trajectories also bring further difficulties to this task.

Previous researchers access this task from two main aspects, i.e., the interactive factors that influence agents' future choices, and the modeling of trajectory itself. Among all kinds of factors, the agent-agent interactions [1], [2] and the agent-object interactions [3], [4] have been widely studied by lots of researchers. Many methods have archived excellent prediction performance by taking these interactive factors into consideration. On the other hand, another group of researchers focuses on exploring the proper way to model trajectories. Neural networks like Long-Short Term Memory Networks (LSTMs), Graph Convolution Networks (GCNs), and Transformers are employed to construct relations inner trajectories. Besides, trajectories' multi-modal characteristics [2], [4] and their goal distribution rules [5], [6] are also explored by several researchers recently.

Although a lot of prediction methods have been proposed and shown great performance, experimental results still show that they have huge evolutionary potential. Especially in recent years, researchers have focused more on modeling the interactive factors that affect agents' future plannings. Few of them have paid more attention to the trajectory itself. In most methods, agents' observed trajectories are treated as time sequences and directly input to neural networks. Different from other time series like audio sequences involved in the signal processing field, the adjacent points in the trajectory sequences will exhibit a stronger correlation due to agents' continuous motions and the physical constraints. It means that processing the trajectory sequences directly will lead to vast information redundancy, which makes networks difficult to notice the truly valuable discriminative information within different trajectories.

Authors are with Huazhong University of Science and Technology, Wuhan, Hubei, P.R.China.

Email: {conghao\_wong, xbh\_hust, pengqinmu, youxg}@hust.edu.cn, hoongzm@gmail.com.

Manuscript received XX XX, XXXX; revised XX XX, XXXX.

We try to address this problem by employing Discrete Fourier Transform in the trajectory prediction task. The Fourier Transform has been applied in many other tasks and achieved great success. It decomposes the time sequences into a series of sinusoids with different frequencies and phases, therefore helping us focus on information that is hard to see in the original sequences. As shown in Fig.1, we show an agent's two-dimensional trajectory in the time series view and the spectrum view. Even if the two trajectory projection sequences in different spatial directions have similar shapes, they show considerable differences in the spectrum view:

- *Intentions and Global Plannings*: The overall trend of agents' observed trajectories will express their future intentions and general plannings roughly. The low-frequency portions in the spectrums of agents' observed trajectories could be able to reflect their overall motion trends. Furthermore, these portions could demonstrate their global future plannings approximately due to the continuity of agents' movements.
- *Interactive Preferences*: Different agents' various interactive preferences are difficult to describe in the time-sequences quantitatively. In most cases, these interactive behaviors will not seriously affect agents' overall future plannings. For example, how long the agent maintains a social distance with others, and within what range does the agent begin to interact with other objects, etc. The high-frequency portions in the spectrums of their observed trajectories will directly show the changing laws of the rapidly changing motions, therefore helping describe their personalized interaction preferences further.

It means that different frequency portions in the trajectory spectrums would be able to reflect different aspects of their activity preferences, i.e., the low-frequency portions could reflect their global motions trends, and the high-frequency portions reflect their interaction preferences. Besides, agents always determine their future activities from two steps. They make a coarse overall motion decision first, and then respond to the potential emergencies (like interactive behaviors) in the future. Inspired by that, a natural thought is to handle spectrums hierarchical, therefore finely modeling and describing agents' behaviors at different levels, i.e., the *coarse* and the *fine* levels, and finally forecasting future trajectories in these levels hierarchically.

In this paper, we propose the V to forecast trajectories in the spectrum view. Our contributions are listed as follows:

- We introduce the Fourier Transform into the trajectory prediction task and try to hierarchically model and forecast agents' trajectories with spectrums.
- A two-stage Transformer-based V network is proposed to implement on trajectory spectrums with both the coarse keypoints estimation and the fine spectrum interpolation sub-networks, therefore predicting trajectories from a "vertical" view.
- Experiments show that V outperforms most current state-of-the-art methods on many public trajectory datasets with about 15% quantitative improvements.

## 2 RELATED WORK

There has been a lot of previous researches aim at forecasting agents' possible future trajectories or behaviors. Many researchers are committed to this task and make their contributions mainly in three aspects, i.e., the modeling of agents' trajectories or behaviors, factors that affect agents' future choices, and the multi-modal characteristics. Although many researchers have explored interactive factors, like social interactions [1], [7], [8], [9] and scene interactions (also called the physical interactions) [3], [4], [10], [11], and how they influence agents' future plannings, the focus of our work lies not here. We discuss existing works on the trajectory prediction topic from the other two aspects.

### 2.1 Trajectory Modeling

Trajectory prediction aims at forecasting agents' possible future trajectories. The modeling of trajectories matters how their prediction networks work directly. Alahi et al. [1] treat this task as a sequence generation problem, and employ the Long-Short Term Memory Network (LSTM) to predict pedestrians' positions in the time step. After that, Huang et al. [7] propose the Spatial-Temporal Graph Attention networks, which gathers LSTMs and graph attention networks to handle interactions and trajectories from time and space two dimensions. It improves the prediction performance by focusing on the most valuable parts with the help of attention mechanism [12]. Mohamed et al. [8] employ the Graph Convolutional Networks (GCN) to process trajectories and interactions, which also show a better prediction performance. Recently, several researchers like [13], [14] have introduced Transformers [12] into this task. Experimental results show their excellent prediction accuracy.

Although these methods use a variety of backbones to model trajectories, most of them implement on the time sequences directly. Some methods try to model the differential trajectories, but they do not obtain considerable performance improvements. In this paper, we try to model agents' trajectories from another view, i.e., model trajectories and behaviors with the Fourier spectrums, thus further exploring the better way to model their trajectories.

### 2.2 Multi-Output Trajectory Prediction

Some researchers address agents' uncertainty and randomness when making decisions by introducing generative models into this task. Agrim et al. [2] use the Generative Adversarial Network (GAN) to generate multiple random trajectories to suit agents' various future choices. Ivanovic et al. [15] employ the Conditional Variation AutoEncoder (CVAE) to achieve a similar goal. In addition to generative models, some methods attribute the uncertainty of agents' activities to the diversity of their destination choices. Mangalam et al. [5] infer distant trajectory endpoints to assist in long-range multi-modal trajectory prediction. Tran et al. [6] try to obtain multi-modal goal proposals from the additional goal channel to help generate multiple predictions. Besides, [16] converts agents' diversity on future trajectories into the multi-style characteristics of their activity styles and preferences, thereby using multiple sets of prediction networks with different styles to obtain multiple future predictions.

These methods have achieved excellent results in generating multiple future predicted trajectories, but most of these methods lack consideration of the actual situation of agents' realistic activity plannings. For example, whether it is a pedestrian, a robot, or a car, the agent always gives a rough trend of future activities and further responds to various emergencies. We try to deal with the diversified future planning of the agent from this kind of consideration. In detail, we try to forecast agents' multiple coarse overall future trends via several keypoints' predictions first, and then employ another sub-network to finish their fine trajectories, thus giving multiple predictions that are in line with social and physical motion rules. Unlike these goal-driven methods, we try to use overall motion trends (i.e., the keypoints) to reflect their overall future planning, thereby reflecting their various planning preferences in detail.

### 3 V

This paper takes the *Fourier Transform* into the trajectory prediction task to view trajectories from another view. The proposed V employs two continuous sub-networks, the coarse *keypoints estimation* and the fine *spectrum interpolation* sub-networks, to archive the prediction goal hierarchically. Fig.2 shows its primary structure. Detailed layer configurations and parameters are listed in Table 1.

#### 3.1 Problem Settings

We assume that we have a video clip  $V = \{I_1, I_2, \dots, I_{t_h}\}$  contains  $N$  agents' observed trajectories  $\mathcal{X} = \{X_1, X_2, \dots, X_N\}$  during the observation period  $T = \{1, 2, \dots, t_h\}$ . Trajectory prediction focused in this research is to predict agents' coordinates  $\hat{\mathcal{Y}} = \{Y_1, Y_2, \dots, Y_N\}$  at the corresponding future  $t_f$  steps based on their previous trajectories  $\mathcal{X}$  and the visual information  $V$ . Formally, we aim at building and training a network  $f$ , such that  $\hat{\mathcal{Y}} = f(\mathcal{X}, V)$ . Let  $p_t = (p_{x_t}, p_{y_t})$  denote the two-dimensional coordinates of each agent at step  $t$ ,  $X = (p_1, p_2, \dots, p_{t_h})$  denote each agents' observed trajectory, and  $Y = (p_{t_h+1}, p_{t_h+2}, \dots, p_{t_h+t_f})$  denote the future trajectory to be forecasted.

#### 3.2 Keypoints Estimation

The coarse keypoints estimation sub-network aims to forecast several key positions on the corresponding future time steps with a *lower spatial-temporal resolution*. It learns agents' behavior patterns from spectrums, making itself available to focus on the behavior details that are difficult to reflect in the time series. In addition, agents' multi-style characteristics [16] are also considered in this stage. A VAE-like encoder-decoder structure is designed to generate multiple random estimations to adapt to agents' uncertainty and randomness.

##### 3.2.1 Embedding

We first employ Discrete Fourier Transform (DFT) on trajectory sequences to obtain the corresponding spectrums. We apply 1D-DFT on each dimension in the trajectory  $X = \{(p_{x_t}, p_{y_t})\}_t$  to obtain the Fourier spectrums, including

the amplitude sequences  $\{a_x, a_y\}$  and the phase sequences  $\{\phi_x, \phi_y\}$ . Formally,

$$\begin{aligned}\mathcal{X} &= \text{DFT}[(p_{x_1}, p_{x_2}, \dots, p_{x_{t_h}})], \\ \mathcal{Y} &= \text{DFT}[(p_{y_1}, p_{y_2}, \dots, p_{y_{t_h}})], \\ a_x &= \|\mathcal{X}\|, \quad a_y = \|\mathcal{Y}\|, \\ \phi_x &= \arg \mathcal{X}, \quad \phi_y = \arg \mathcal{Y}.\end{aligned}\tag{1}$$

We employ a trajectory embedding MLP named TE (see detailed structure in Table 1) to embed agents' observed trajectories (spectrums) into the high-dimension  $f_t$ :

$$f_t = \text{TE}([a_x, a_y, \phi_x, \phi_y]) \in \mathbb{R}^{t_h \times 64},\tag{2}$$

where  $[a, b, \dots]$  represents the concatenation operation. Similarly, we use a context embedding MLP (CE in Table 1) to embed the scene context map  $C$  [16] (which encodes both social interactions and scene constraints together) into the context feature  $f_c$ :

$$f_c = \text{CE}(C) \in \mathbb{R}^{t_h \times 64}.\tag{3}$$

Then, we combine the above representations to obtain the embedded vector:

$$f_e = [f_t, f_c] \in \mathbb{R}^{t_h \times 128}.\tag{4}$$

##### 3.2.2 Multi-Style Features Encoding

We use a Transformer-based sub-network to encode agents' behavior features. The embedded vector  $f_e$  is passed to the Transformer encoder [12], and the spectrum sequences  $\{a_x, a_y, \phi_x, \phi_y\}$  are passed to the Transformer decoder [12], correspondingly. We pickle vectors (marked with  $f_{tra}$ ) output from the penultimate layer of the Transformer decoder whose shapes are  $t_h \times 128$  as the behavior features (see Table 1 for details).

Following [16], we employ the graph convolution operation [17] to aggregate features at different frequency nodes in  $f_{tra}$ , and use them to represent  $K_c$  styles of multiple activity features  $f_{K_c}$  to suit agents' multiple decision styles. Formally,

$$\begin{aligned}f_{K_c} &= (f_1, \dots, f_k, \dots, f_{K_c})^T \\ &= \text{GraphConv}(f_{tra}, A) \in \mathbb{R}^{K_c \times 128},\end{aligned}\tag{5}$$

where  $A \in \mathbb{R}^{K_c \times t_h}$  is the trainable adjacency matrix.

We concatenate all these operations or layers as an encoder layer EN. See detailed structures in Table 1.

##### 3.2.3 Keypoints Estimation

The coarse keypoints estimation sub-network focuses on forecasting trajectories with a low spatial-temporal resolution. It concerns more about the establishment of agents' overall movements rather than those fine interaction details. We employ an MLP (called the keypoints decoder, KD, in Table 1) to predict coordinates at several "key" future steps. Let  $N_{key}$  be the number of these keypoints, and we have the estimated keypoints  $\hat{y}^{key}$  under the  $k$ -th style:

$$\begin{aligned}(a_{xk}^{key}, a_{yk}^{key}, \phi_{xk}^{key}, \phi_{yk}^{key}) &= \text{KD}(f_k) \in \mathbb{R}^{N_{key} \times 4}, \\ \mathcal{X}^{key} &= a_{xk}^{key} \exp(j\phi_{xk}^{key}), \\ \mathcal{Y}^{key} &= a_{yk}^{key} \exp(j\phi_{yk}^{key}), \\ \hat{y}_k^{key} &= (\text{IDFT}[\mathcal{X}^{key}], \text{IDFT}[\mathcal{Y}^{key}]).\end{aligned}\tag{6}$$

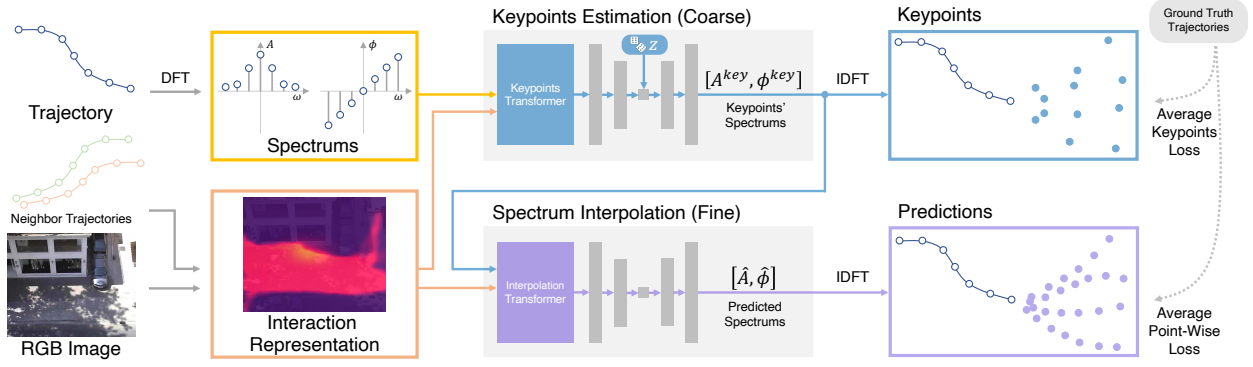


Fig. 2. V Overview. It contains two main sub-networks, the coarse keypoints estimation sub-network and the fine spectrum interpolation sub-network. Both of them implement on spectrums of observed trajectories, thus giving multiple future predictions hierarchically.

We have the estimated keypoints after repeating the above process on all styles' features  $f_k \in (f_1, \dots, f_{K_c})$ . The KL loss is applied on the latent feature  $f_k$ . It forces these features to distribute similarly enough to the specific distribution (the normalized Gaussian distribution). Thus, the keypoints decoder could output stochastic predictions by adding the randomly sampled noise vector  $z \sim \mathcal{N}(0, I)$ . It makes the predictions in line with agents' uncertainty of the overall future plans and the multi-style characteristics of their behavior preferences.

### 3.3 Spectrum Interpolation

We obtain coordinates at all prediction moments by the fine spectrum interpolation sub-network, which reconstructs trajectories from keypoints sequences with a *higher spatial-temporal resolution* based on the spectrums.

Similar to the keypoints estimation, we apply the 1D-DFT on each dimension of trajectory sequences to let the sub-network learn the spectrum biases between actual trajectory sequences and the predicted keypoints sequences. For the amplitude and phase sequences in Equation 6, we have the representation of the keypoint sequences:

$$f_t^{key} = \text{TE}([a_{xk}^{key}, a_{yk}^{key}, \phi_{xk}^{key}, \phi_{yk}^{key}]) \in \mathbb{R}^{N_{key} \times 64}. \quad (7)$$

We employ a similar Transformer-based sub-network (called the Interpolation, IP) to learn the relationship in spectrums between the keypoints and their realistic trajectories. We pass the  $f_e^{key} = [f_t^{key}, \text{CE}(C)]$  to the transformer encoder, and the spectrum sequences  $[a_{xk}^{key}, a_{yk}^{key}, \phi_{xk}^{key}, \phi_{yk}^{key}]$  to the transformer decoder. It is designed to output the predicted spectrum sequences. Formally,

$$[\hat{a}_x, \hat{a}_y, \hat{\phi}_x, \hat{\phi}_y] = \text{IP}(f_e^{key}, [a_{xk}^{key}, a_{yk}^{key}, \phi_{xk}^{key}, \phi_{yk}^{key}]). \quad (8)$$

The IDFT is applied to obtain the corresponding time-sequences  $\hat{y}_o$ . Formally,

$$\begin{aligned} \hat{\mathcal{X}} &= \hat{a}_x \exp(j\hat{\phi}_x), \quad \hat{\mathcal{Y}} = \hat{a}_y \exp(j\hat{\phi}_y), \\ \hat{y}_o &= (\text{IDFT}[\hat{\mathcal{X}}], \text{IDFT}[\hat{\mathcal{Y}}]). \end{aligned} \quad (9)$$

The  $\hat{y}_o \in \mathbb{R}^{(t_h+t_f) \times 2}$  contains both the reconstructed observed trajectory and the predicted trajectory. Finally, we have one of the V predictions

$$\hat{y} = \hat{y}_o[t_h :, :], \quad (10)$$

where the  $[t_h :, :]$  indicates the slicing operation on tensors.

### 3.4 Loss Functions

We use the following loss function to train the V:

$$\begin{aligned} \mathcal{L} = & \underbrace{\mu_1 \min_k \|y_k^{key} - \hat{y}_k^{key}\|_2}_{\text{AKL}} + \underbrace{\mu_2 \text{KL}(P(f_k) \| \mathcal{N}(0, I))}_{\text{KL Loss}} + \\ & \underbrace{\mu_3 \|\hat{y} - y\|_2}_{\text{APL}}, \end{aligned} \quad (11)$$

where  $\{\mu_1, \mu_2, \mu_3\}$  is a set of balance parameters. The KL Loss term is used for training the encoder-decoder structure in keypoints estimation sub-network to generate multiple stochastic predictions. Other loss function terms and their optimization goals are listed below:

(a) **AKL** indicates the Average Keypoints Loss. It is the average minimum point-wise  $\ell_2$  distance among keypoints and their predictions. It is used to train variables in the keypoints estimation sub-network.

(b) **APL** indicates the Average Point-wise Loss. It is the average point-wise  $\ell_2$  distance among the entire future trajectory and the prediction. We use this loss function to train variables in the spectrum interpolation sub-network.

## 4 EXPERIMENTS

### 4.1 Experimental Setup

#### 4.1.1 Datasets

We evaluate V on three public trajectory datasets, ETH [18], UCY [19], and Stanford Drone Dataset (SDD) [20]. They are consist of a number of agents' trajectories with rich social interactions and scene constraints in various scenarios.

TABLE 1  
Architecture details of the proposed V.

Layers	Structure
TE	$\rightarrow 64 \rightarrow \text{ReLU} \rightarrow 64 \rightarrow \tanh \rightarrow$
CE	$\rightarrow \text{MaxPooling} (5 \times 5) \rightarrow \text{Flatten} \rightarrow 64t_h \rightarrow \tanh \rightarrow \text{Reshape} (t_h \times 64) \rightarrow$
EN	$\rightarrow \text{TransformerEncoder} (128) \rightarrow \text{TransformerDecoder} (128) \rightarrow \text{GraphConv} (128) \rightarrow$
KD	$\rightarrow 128 \rightarrow \text{ReLU} \rightarrow 128 \rightarrow \text{ReLU} \rightarrow 4N_k \rightarrow \text{Reshape} (N_{key} \times 4) \rightarrow$
IP	$\rightarrow \text{TransformerEncoder} (128) \rightarrow \text{TransformerDecoder} (4) \rightarrow$

(a) **The ETH-UCY Benchmark:** Many previous methods [1], [2], [3] take several sub-datasets from ETH and UCY (eth and hotel from the ETH dataset, plus univ, zara1, zara2 from the UCY dataset) to train and evaluate their models with the “leave-one-out” strategy, which is called the ETH-UCY benchmark. It contains 1536 pedestrians in total with thousands of non-linear trajectories. The annotations are pedestrians’ real-world coordinates in meters.

(b) **Stanford Drone Dataset:** The Stanford Drone Dataset (SDD) is a popular computer vision dataset. It can be used in object detection, tracking, trajectory prediction, and many other tasks. More and more trajectory prediction models have started to validate their models on it. It has 60 bird-view videos captured by drones over the Stanford campus. More than 11,000 different kinds of agents are annotated with bounding boxes in pixels. It contains over 185,000 social behaviors and 40,000 interactive scene behaviors.

#### 4.1.2 Metrics

We employ two metrics to evaluating the prediction accuracy, including the Average Displacement Error (ADE) and the Final Displacement Error (FDE) [18].

(a) **ADE:** It is the average point-wise Euclidean distance between groundtruth and predictions of all steps. For one prediction smaple, we have

$$\text{ADE}(y, \hat{y}) = \frac{1}{t_f} \sum_t \|p_t - \hat{p}_t\|_2. \quad (12)$$

(b) **FDE:** It is the Euclidean distance between the last point’s prediction and groundtruth. Formally,

$$\text{FDE}(y, \hat{y}) = \|p_{t_h+t_f} - \hat{p}_{t_h+t_f}\|_2. \quad (13)$$

#### 4.1.3 Baselines

We choose several state-of-the-art methods as our baselines. They are:

- **Social GAN** [2]: A GAN-based model that guides the pooling mechanism to model social interaction.
- **SoPhie** [3]: An attentive GAN-based model that considering both social interaction and scene context.
- **Social-BiGAT** [4]: A model that takes Bicycle-GAN and graph representation to model interactions.
- **Multiverse** [21]: A model that focuses on predicting the distribution over multiple possible future paths of people moving through various visual scenes.
- **SimAug** [22]: A model that builds additional multi-view simulation datasets to solve different views.
- **PECNet** [5]: A goal-conditioned prediction model that divides the task into goal and trajectory stages.
- **TPNMS** [23]: A model that builds a feature pyramid with increasingly richer temporal information to capture agents’ motion behavior at various tempos.
- **E-SR-LSTM** [24]: A model that exploits spatial-edge LSTMs to enhance the interaction-modeling capacity.
- **TP** [13]: A Transformer-based model that reaches excellent performance without considering interactions.
- **Trajectron++** [25]: A recurrent-graph based model that aims at catching agents and scene dynamic constraints.

- **Introvert** [26]: An LSTM-based model that infers both environmental constraints and social interactions through observing the dynamic scene instead of communicating with other humans.
- **LB-EBM** [27]: A probabilistic cost model in the latent space accounting for movement history and social context.
- **MSN** [16]: A model that employs predictors with various “styles” for the same agent to obtain multi-style predictions.

#### 4.1.4 Implementation Details

We predict agents’ trajectories in future  $t_f = 12$  frames according to their  $t_h = 8$  frames’ observations. We train the entire V with the Adam optimizer (learning rate  $\text{lr} = 0.0003$ ) on the NVIDIA Tesla P4 graphic processor. The V is trained with the batch size  $\text{bs} = 2000$  for 800 epochs on ETH-UCY and 150 epochs on SDD. When training and validating models, we follow the “leave-one-out” strategy [2] on ETH-UCY and use the same dataset splits as [22] on SDD. The frame rate is set to 2.5 frames per second when sampling trajectories. Detailed layer connections, output units, and activations are listed in Table 1. Following [16], the number of behavior styles is set to  $K_c = 20$ . Balance coefficients used in loss functions are set to  $\{\mu_1, \mu_2, \mu_3\} = \{0.5, 1.0, 0.5\}$ . The number of keypoints is set to  $N_{key} = 3$ , and their time steps are set to  $\{t_{k1}, t_{k2}, t_{k3}\} = \{t_{h+4}, t_{h+8}, t_{h+12}\}$ . (Only for prediction cases when  $t_h = 8$  and  $t_f = 12$ .)

## 4.2 Comparison to State-of-the-Art Methods

We show the quantitative performance comparisons with several state-of-the-art methods in Table 2. Metrics are displayed in the form of “ADE/FDE” with the “best-of-20” evaluation method ([2], [3], [25]). Note that metrics are shown in meters on the ETH-UCY benchmark and pixels on SDD. A lower value indicates a better prediction accuracy.

#### 4.2.1 ETH-UCY Benchmark

As shown in Table 2, V achieves superior performance compared to a lot of state-of-the-art methods on most sub-datasets on ETH-UCY. It improves the metrics on eth for over 26.6% and 32.6% compared with the state-of-the-art LB-EBM. Similarly, V outperforms the state-of-the-art Introvert on hotel by about 10.0% ADE and 11.7% FDE. Besides, V has achieved comparable performance to the state-of-the-art Introvert on the zara1 and zara2 sub-datasets. Although V’s performance on univ is slightly worse than others, it still greatly exceeds other methods in the average performance of all ETH-UCY sub-datasets. Compared with the current state-of-the-art Introvert, its average ADE has improved over 14.2%, and FDE over 14.7%. It shows V’s superior average performance on ETH-UCY.

#### 4.2.2 SDD

V also has a better performance improvement than a lot of previous state-of-the-art methods on SDD. Compared with the state-of-the-art LB-EBM, the ADE has been improved for over 17.2%, and the FDE has been extremely improved for over 26.1%. Even compared with the con-current MSN, V also have a performance improvement for 4.42% and



TABLE 2  
Comparisons with the *best-of-20* validation. Metrics are shown in the format of “ADE/FDE”. Lower means better.

Model	eth	hotel	univ	zara1	zara2	Average
Social GAN [2]	0.60/1.19	0.52/1.02	0.44/0.84	0.22/0.43	0.29/0.58	0.41/0.81
SoPhie [3]	0.70/0.43	0.76/1.67	0.54/1.24	0.30/0.63	0.38/0.78	0.54/1.15
Social-BiGAT [4]	0.69/1.29	0.49/1.01	0.55/1.32	0.30/0.62	0.36/0.75	0.48/1.00
PECNet [5]	0.54/0.87	0.18/0.24	0.35/0.60	0.22/0.39	0.17/0.30	0.29/0.48
TPNMS [23]	0.52/0.89	0.22/0.39	0.55/0.13	0.35/0.70	0.27/0.56	0.38/0.73
E-SR-LSTM [24]	0.44/0.79	0.19/0.31	0.50/1.05	0.32/0.64	0.27/0.54	0.43/0.67
TP [13]	0.61/1.12	0.18/0.30	0.35/0.65	0.22/0.38	0.17/0.32	0.31/0.55
Trajectron++ [25]	0.43/0.86	0.12/0.19	0.22/0.43	<b>0.17/0.32</b>	<b>0.12/0.25</b>	0.20/0.39
Introvert [26]	0.42/0.70	<b>0.11/0.17</b>	<b>0.20/0.32</b>	<b>0.16/0.27</b>	0.16/ <b>0.25</b>	0.21/0.34
LB-EBM [27]	0.30/0.52	0.13/0.20	0.27/0.52	0.20/0.37	0.15/0.29	0.21/0.38
MSN [16]	0.27/0.41	<b>0.11/0.17</b>	0.28/0.48	0.22/0.36	0.18/0.29	0.21/0.34
V (Ours)	<b>0.22/0.35</b>	<b>0.10/0.15</b>	0.26/0.44	<b>0.17/0.29</b>	0.15/ <b>0.24</b>	<b>0.18/0.29</b>

Models	Social GAN	SoPhie	Multiverse [21]	SimAug [22]	PECNet	LB-EBM	MSN	V (Ours)
SDD	27.25/41.44	16.27/29.38	14.78/27.09	12.03/23.98	9.96/15.88	8.87/15.61	7.68/12.16	<b>7.34/11.53</b>

5.18%. In general, V has a better prediction accuracy on SDD than most current state-of-the-art methods.

## 4.3 Discusses

### 4.3.1 Ablation Studies

We design several model variations and run ablation studies to verify each component in the proposed V. Quantitative results are shown in Table 3. Note that all variations are validated under the *best-of-20* validation.

**a. Spectrum** V implements on the spectrums to focus on different frequencies in different prediction stages, thus better modeling agents’ various behaviors. Ablation variations a1 and a2 are trained with the same number of keypoints  $N_{key} = 1$ , while a1 do not implement with DFT/IDFT when predicting. The only difference between a1 and a2 is that a2 obtains behavior features and interaction features from the spectrums, and a1 obtains from the time sequences. Experiments show that a2 outperforms a1 for over 10% ADE and FDE on ETH-UCY. It demonstrates the performance improvement bring by the spectrums.

**b. Number of Keypoints** The number of keypoints  $N_{key}$  matters how the keypoints estimation stage sub-network determines agents’ styles of their future behaviors. It gives all agents multiple keypoints estimations within several different styles. In other words, it “judges” agents’ behavior styles through these keypoints. A small  $N_{key}$  value will result in too loose style division, making it challenging to reflect the differences between different styles. However, a larger value may result in a strict style division, making it difficult to reflect agents’ multi-style future choices. Experiments on variations a2, b1, and b2 show the quantitative comparisons with different  $N_{key}$  configurations. It shows that the b1 ( $N_{key} = 3$ ) outperforms a2 ( $N_{key} = 1$ ) with additional improvements for about 5% ADE and 6% FDE. However, The performance of b2 ( $N_{key} = 6$ ) reduces by about 1% to 5% compared to the basic variation a1. Please see visualized trajectories of different  $N_{key}$  variations in section 4.3.2b to learn how they affect the prediction performance qualitatively.

**c. Spectrum Interpolation** The V splits trajectory prediction into a two-stage “keypoints-interpolation” process. Although the first stage sub-networks have already given a low-resolution prediction composed of a few keypoints, they are difficult to reflect agents’ subtle interaction and activity differences. Ablation variations b1 and c show the improvements brought by the second-stage interpolation sub-networks. Results show that the spectrum interpolation improves over 10% ADE to the variation c (which takes the linear interpolation as the second-stage interpolation method). It effectively proves the superiority of the spectrum interpolation network for describing and modeling agents’ fine activities.

**d. Verifying of  $k$**  Similar to MSN [16], the proposed V gives multiple predictions in a multi-style way. In this section, we verify the performance improvement to the MSN when generating a large number of stochastic predictions. See details in Table 4. It shows that the V outperforms MSN up to 50% FDE and 30% ADE when outputting 1000 trajectories. Besides, V’s prediction accuracy increases more as the number of stochastic predictions generated increases.

### 4.3.2 Qualitative Analysis

We have also designed some qualitative analyses to verify how each design works on the predicted trajectories.

**a. Keypoints and Interpolation** One of the key ideas in the V is to predict agents’ multiple future keypoints at the first stage and then use an interpolation method to give the entire prediction. Fig.3 shows two prediction examples at keypoints estimation and spectrum interpolation stages correspondingly. At the first stage, V estimates positions on several future key time steps (shown in the first row in Fig.3). It should be noted that we designed this stage to obtain predictions with a low spatial and temporal resolution. It means that these critical points only represent the general trend of the agent’s future activities rather than specific coordinates.

As shown in Fig.3 (a) and (b), predictions at the keypoints stage show how these two pedestrians could move in the future globally, and then the final predictions after

TABLE 3

Ablation Studies: ADE and FDE on ETH-UCY benchmark. S1 and S2 represent the keypoints prediction stage and the spectrum interpolation stage, correspondingly. Spectrum indicates whether methods model trajectories with spectrums or the time-sequences.  $N_{key}$  is the number of keypoints used in methods. Results in “↑” are the metric improvements compared to a1.

No.	S1	S2	Spectrum	$N_{key}$	eth	hotel	univ	zara1	zara2	Average	↑(%)
a1 (MSN [16])	✓	✓	×	1	0.28/0.44	0.11/0.17	0.28/0.48	0.22/0.36	0.18/0.29	0.21/0.35	- (base)
a2	✓	✓	✓	1	0.22/0.37	0.11/0.16	0.29/0.46	0.20/0.31	0.17/0.26	0.19/0.31	10%/12%
b1	✓	✓	✓	3	0.22/0.35	0.10/0.15	0.26/0.44	0.17/0.29	0.15/0.24	0.18/0.29	15%/18%
b2	✓	✓	✓	6	0.28/0.46	0.12/0.16	0.28/0.48	0.23/0.36	0.22/0.31	0.22/0.36	-5%/-1%
c	✓	linear	✓	3	0.23/0.35	0.11/0.15	0.28/0.44	0.19/0.29	0.16/0.25	0.20/0.30	5%/15%

TABLE 4

Verifying of  $k$ . Metrics are shown with “ADE/FDE”. “%” are improvements compared to MSN with the same other configurations.

	$K_c$	$k$	Ours	MSN	↑(%)
ETH-UCY	20	5	0.14/0.17	0.16/0.23	12.3% / 24.8%
	20	10	0.12/0.12	0.15/0.20	20.1% / 34.6%
	20	20	0.10/0.09	0.14/0.17	24.5% / 44.1%
	20	30	0.10/0.07	0.13/0.15	26.8% / 46.7%
	20	50	0.09/0.06	0.13/0.13	31.4% / 51.2%
SDD	20	5	5.80/6.90	5.83/7.93	0.5% / 12.9%
	20	10	4.95/4.95	5.27/6.49	6.0% / 23.6%
	20	20	4.30/3.52	4.86/5.30	11.5% / 33.6%
	20	30	3.98/2.87	4.68/4.71	14.8% / 38.9%
	20	50	3.67/2.28	4.46/4.03	17.5% / 43.4%

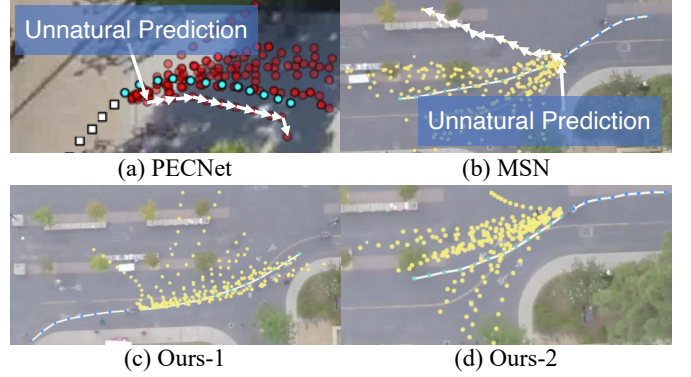


Fig. 5. Smoothness Comparisons. (a) and (b) are visualized predictions pickled from PECNet [5] and MSN [16], and (c)(d) are predictions given by V. With the help of spectrums, V’s predictions show better continuous and smoothness.

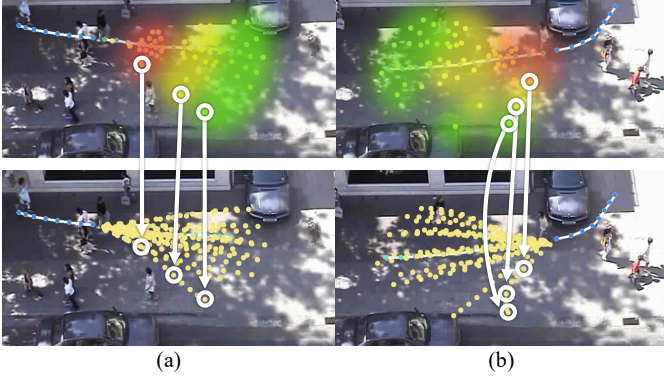


Fig. 3. Keypoints and Interpolation Illustration. We show the predicted keypoints ( $N_{key} = 3$ ) in the first row. Their corresponding time steps are distinguished with different color masks. Figures in the second row show the entire predicted trajectories after spectrum interpolation. Dots marked with white circles are the same prediction at these two stages.

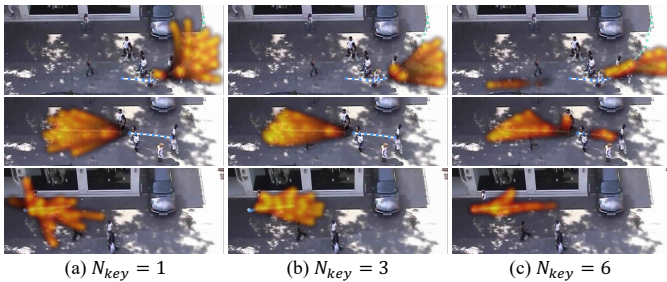


Fig. 4. Number of Keypoints and Stylized Prediction Illustration. We show the visualized V results with  $N_{key} = \{1, 3, 6\}$  in the distribution way. Yellow represents the area has more predicted dots given by V, and red represents less.

the interpolation stage consider both physical constraints and social interactions to fine-tune these keypoints. For example, the marked keypoints in Fig.3(b) indicate that the pedestrian could go toward the road. On the contrary, the corresponding final prediction shows that he might slow down and stay on the side of the road considering the scene’s physical constraints.

**b. Number of Keypoints and Prediction Styles** We estimate agents’ future keypoints to determine their coarse future routes. At the same time, we will train the prediction network adaptively according to the keypoints’ distribution, therefore giving multi-style keypoints to adapt to agents’ uncertain future decisions. In other words, these keypoints are the indicator for us to judge which kind of behavior styles some trajectories could be. The number of keypoints matters directly V’s multi-output performance, which can be seen in Fig.4.

It shows that Fig.4(a) exhibits a looser restraint when generating trajectories. Obviously, it is caused by the insufficient stylized constraints from the keypoints. Although (a) gives a large number of future predictions, most of them may be invalid or do not meet the scene constraints. Visualized results indicate that V will give more rigorous predictions as the number of keypoints ( $N_{key}$ ) increases. It gives more acceptable predictions when setting the  $N_{key} = 3$  (Fig.4(b)). However, its predictions will be limited to a small area when  $N_{key}$  is set to 6 (Fig.4(c)). V will hardly reflect agents’ realistic multi-style planning preferences under the constraints of such excessive keypoints. It explains the drop of quantitative performance when setting  $N_{key}$  to 6 in the

above ablation studies.

**c. Smoothness** In earlier studies on trajectory prediction, researchers have widely used *autoregressive models*, such as recurrent neural network (RNN) [28] and long-short term memory (LSTM) [1], to forecast agents' future trajectories "step-by-step". They model agents' behaviors and interactions in the next step based on their last observed states. These models could better describe the state changes between the adjacent moments. Therefore, their predicted trajectories reflect better smoothness characteristics. However, more and more *non-autoregressive models* like [5], [13], [16] are proposed and show excellent quantitative results. These models predict agents' positions at different future moments in parallel, which means that the relationship between predicted dots has been less concerned.

Fig.5(a) and (b) are visualized trajectories pickled from [5] and [16]. Although these methods have achieved good qualitative prediction performance, some of their predictions do not seem so "continuous". With the help of the spectrum interpolation, V could give "smoother" predictions than these models. In other words, the V predicts agents' spectrums directly, rather than the time-sequences. It means that in the IDFT process, the correlation between adjacent time steps will be smoothly constrained via sinusoids. Fig.5(c) and (d) show the relatively smooth predicted trajectories given by V. It better reflects agents' real motion laws due to physical movement limitations.

**d. Visualization** We display several predicted trajectories on both ETH-UCY and SDD to show performance qualitatively. As shown in Fig.6, V could give multiple possible trajectories to most agents under the control of scene constraints and social interactions. For example, V gives a variety of different future options for bikers who are about to pass the crossroads (shown in Fig.6(a)(e)(k)). In particular, in the prediction case (e) and (k), the model takes into account the physical constraints of the environment and gives a prediction that bypasses the grass.

In addition, it also shows strong adaptability in some unique prediction scenarios. For example, it gives three different styles of predictions to the biker in case (h) to pass through the traffic circle: turning right, going ahead, and turning left. In the case of turning left, the given predictions are not to turn directly to the left (just like turning right) but to go left after going around the circle, which is strongly consistent with the traffic rules around the circle. Prediction case (i) shows the similar trends for the man who are passing the crossroads. It shows V could accurately describe the scene's physical constraints and agents' motion rules in various prediction scenes.

#### 4.4 Failure Cases

Although the proposed V shows several qualitative and quantitative advantages, it still has failure prediction cases. V has failed predictions for (almost) stationary agents, which can be seen in Fig.7. Although not all 20 predictions are regarded as failed predictions, some of them show quite unreasonable movement trends for these standing still agents. We will try to fix this problem in our future works.

## 5 CONCLUSION

In this work, we focus on predicting agents' trajectories in the spectrum view hierarchically. A Transformer-based V network is proposed to achieve that goal. Two sub-networks, the keypoints estimation sub-network and the spectrum interpolation sub-network, are employed to predict agents' trajectories in keypoints levels and interaction levels, respectively. Experimental results show that V outperforms most of current state-of-the-art methods on several public available trajectory datasets with about 15% improvements on ADE and FDE. Although the proposed method shows higher prediction accuracy and has better visualized results than other methods, there are still some failed predictions. We will try to address this problem in future works and further explore better methods to model and predict agents' possible trajectories.

## REFERENCES

- [1] A. Alahi, K. Goel, V. Ramanathan, A. Robicquet, L. Fei-Fei, and S. Savarese, "Social lstm: Human trajectory prediction in crowded spaces," in *Proceedings of the IEEE conference on computer vision and pattern recognition*, 2016, pp. 961–971.
- [2] A. Gupta, J. Johnson, L. Fei-Fei, S. Savarese, and A. Alahi, "Social gan: Socially acceptable trajectories with generative adversarial networks," in *Proceedings of the IEEE Conference on Computer Vision and Pattern Recognition*, 2018, pp. 2255–2264.
- [3] A. Sadeghian, V. Kosaraju, A. Sadeghian, N. Hirose, H. Rezatofighi, and S. Savarese, "Sophie: An attentive gan for predicting paths compliant to social and physical constraints," in *Proceedings of the IEEE Conference on Computer Vision and Pattern Recognition*, 2019, pp. 1349–1358.
- [4] V. Kosaraju, A. Sadeghian, R. Martín-Martín, I. Reid, H. Rezatofighi, and S. Savarese, "Social-bigat: Multimodal trajectory forecasting using bicycle-gan and graph attention networks," in *Advances in Neural Information Processing Systems*, 2019, pp. 137–146.
- [5] K. Mangalam, H. Girase, S. Agarwal, K.-H. Lee, E. Adeli, J. Malik, and A. Gaidon, "It is not the journey but the destination: End-point conditioned trajectory prediction," in *European Conference on Computer Vision*, 2020, pp. 759–776.
- [6] H. Tran, V. Le, and T. Tran, "Goal-driven long-term trajectory prediction," in *Proceedings of the IEEE/CVF Winter Conference on Applications of Computer Vision*, 2021, pp. 796–805.
- [7] Y. Huang, H. Bi, Z. Li, T. Mao, and Z. Wang, "Stgat: Modeling spatial-temporal interactions for human trajectory prediction," in *Proceedings of the IEEE International Conference on Computer Vision*, 2019, pp. 6272–6281.
- [8] A. Mohamed, K. Qian, M. Elhoseiny, and C. Claudel, "Social-stgcnn: A social spatio-temporal graph convolutional neural network for human trajectory prediction," in *Proceedings of the IEEE/CVF Conference on Computer Vision and Pattern Recognition*, 2020, pp. 14 424–14 432.
- [9] P. Zhang, W. Ouyang, P. Zhang, J. Xue, and N. Zheng, "Sr-lstm: State refinement for lstm towards pedestrian trajectory prediction," in *Proceedings of the IEEE Conference on Computer Vision and Pattern Recognition*, 2019, pp. 12 085–12 094.
- [10] H. Xue, D. Q. Huynh, and M. Reynolds, "Ss-lstm: A hierarchical lstm model for pedestrian trajectory prediction," in *2018 IEEE Winter Conference on Applications of Computer Vision (WACV)*. IEEE, 2018, pp. 1186–1194.
- [11] H. Manh and G. Alaghband, "Scene-lstm: A model for human trajectory prediction," *arXiv preprint arXiv:1808.04018*, 2018.
- [12] A. Vaswani, N. Shazeer, N. Parmar, J. Uszkoreit, L. Jones, A. N. Gomez, L. Kaiser, and I. Polosukhin, "Attention is all you need," in *Advances in neural information processing systems*, 2017, pp. 5998–6008.
- [13] F. Giuliari, I. Hasan, M. Cristani, and F. Galasso, "Transformer networks for trajectory forecasting," pp. 10 335–10 342, 2021.
- [14] C. Yu, X. Ma, J. Ren, H. Zhao, and S. Yi, "Spatio-temporal graph transformer networks for pedestrian trajectory prediction," in *European Conference on Computer Vision*. Springer, 2020, pp. 507–523.



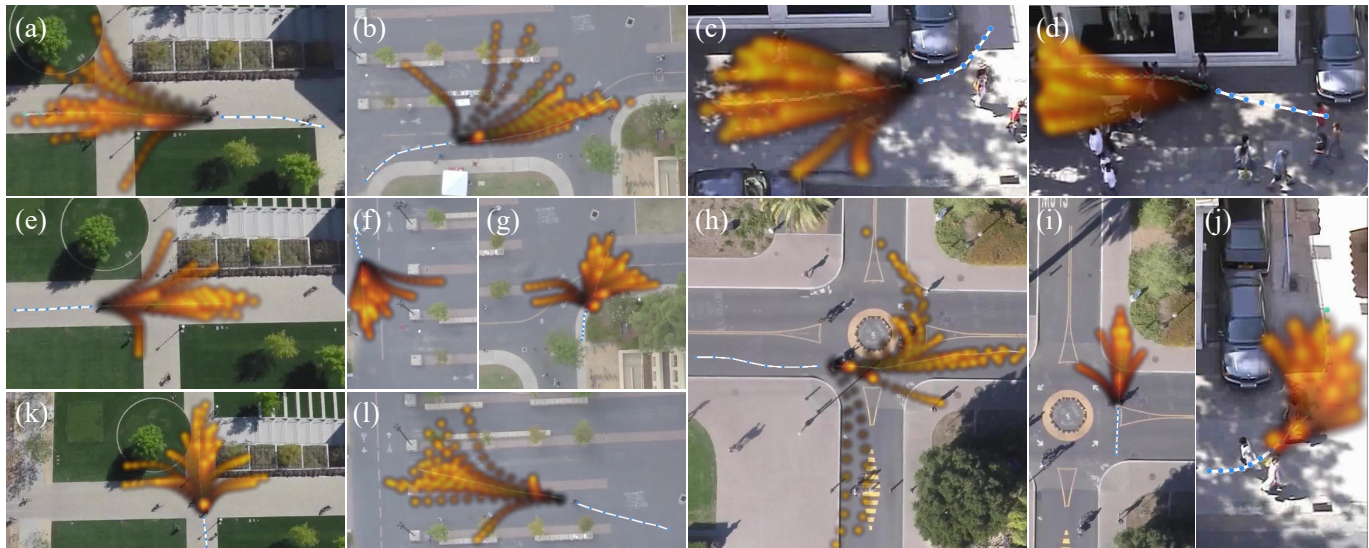


Fig. 6. Visualized Predictions. We draw visualized prediction results with the heatmap form. Each prediction case have  $N = 20$  predictions. Dark colors indicate small time steps, and light colors indicate further future.



Fig. 7. Failure Prediction Cases. V could give several unreasonable predictions to agents who are standing still or moving within a tiny distance.

- [15] B. Ivanovic and M. Pavone, "The trajctron: Probabilistic multi-agent trajectory modeling with dynamic spatiotemporal graphs," in *Proceedings of the IEEE International Conference on Computer Vision*, 2019, pp. 2375–2384.
- [16] C. Wong, B. Xia, Q. Peng, and X. You, "Msn: Multi-style network for trajectory prediction," *arXiv preprint arXiv:2107.00932*, 2021.
- [17] T. N. Kipf and M. Welling, "Semi-supervised classification with graph convolutional networks," *arXiv preprint arXiv:1609.02907*, 2016.
- [18] S. Pellegrini, A. Ess, K. Schindler, and L. Van Gool, "You'll never walk alone: Modeling social behavior for multi-target tracking," in *2009 IEEE 12th International Conference on Computer Vision*. IEEE, 2009, pp. 261–268.
- [19] A. Lerner, Y. Chrysanthou, and D. Lischinski, "Crowds by example," *Computer Graphics Forum*, vol. 26, no. 3, pp. 655–664, 2007.
- [20] A. Robicquet, A. Sadeghian, A. Alahi, and S. Savarese, "Learning social etiquette: Human trajectory understanding in crowded scenes," in *European conference on computer vision*. Springer, 2016, pp. 549–565.
- [21] J. Liang, L. Jiang, K. Murphy, T. Yu, and A. Hauptmann, "The garden of forking paths: Towards multi-future trajectory prediction," in *Proceedings of the IEEE/CVF Conference on Computer Vision and Pattern Recognition*, 2020, pp. 10 508–10 518.
- [22] J. Liang, L. Jiang, and A. Hauptmann, "Simaug: Learning robust representations from simulation for trajectory prediction," in *Proceedings of the European conference on computer vision (ECCV)*, August 2020.
- [23] R. Liang, Y. Li, X. Li, J. Zhou, W. Zou *et al.*, "Temporal pyramid network for pedestrian trajectory prediction with multi-supervision," *arXiv preprint arXiv:2012.01884*, 2020.
- [24] P. Zhang, J. Xue, P. Zhang, N. Zheng, and W. Ouyang, "Social-

aware pedestrian trajectory prediction via states refinement lstm," *IEEE transactions on pattern analysis and machine intelligence*, 2020.

- [25] T. Salzmann, B. Ivanovic, P. Chakravarty, and M. Pavone, "Trajectron++: Dynamically-feasible trajectory forecasting with heterogeneous data," in *Computer Vision–ECCV 2020: 16th European Conference, Glasgow, UK, August 23–28, 2020, Proceedings, Part XVIII 16*. Springer, 2020, pp. 683–700.
- [26] N. Shafiee, T. Padir, and E. Elhamifar, "Introvert: Human trajectory prediction via conditional 3d attention," in *Proceedings of the IEEE/CVF Conference on Computer Vision and Pattern Recognition*, 2021, pp. 16 815–16 825.
- [27] B. Pang, T. Zhao, X. Xie, and Y. N. Wu, "Trajectory prediction with latent belief energy-based model," in *Proceedings of the IEEE/CVF Conference on Computer Vision and Pattern Recognition*, 2021, pp. 11 814–11 824.
- [28] A. Jain, A. R. Zamir, S. Savarese, and A. Saxena, "Structural-rnn: Deep learning on spatio-temporal graphs," in *Proceedings of the IEEE conference on computer vision and pattern recognition*, 2016, pp. 5308–5317.